Extended Simulations for the Link Stress and Elevation Control of a Tethered Aerial Robot

Marco Tognon, Antonio Franchi

Extended Simulations for the Link Stress and Elevation Control of a Tethered Aerial Robot

Technical Attachment to:
"Nonlinear Observer-based Tracking Control of Link Stress and Elevation for a Tethered Aerial Robot using Inertial-only Measurements"
presented at *2015 IEEE Intern. Conf. on Robotics and Automation (ICRA), Seattle WA, May 2015*

Marco Tognon and Antonio Franchi

This document is a technical attachment to [1] as an extension of the simulation's section.

VII. EXTENDED SIMULATIONS

We want to show here some additional simulations of the closed loop system for a better validation of the proposed method. In the following we present the results with different type of references for both the outputs, i.e., *A)* step, *B)* smooth step, *C)* and sinusoidal.

The simulation are done using Simulink and modeling the system with the toolbox *SimMechanics*, thus obtaining a more realistic validation independently from the model used for the control and observer design. The parameters used for these simulations are the same presented in Sec. V of [1], i.e., aerial robot mass: $m_R = 1\,[\mathrm{Kg}]$; moment of inertia $J_R = 0.15\,[\mathrm{Kg\,m^2}]$; link length: $l = 2\,[\mathrm{m}]$; gains $\mathbf{k}_1$ and $\mathbf{k}_2$ chosen such that the poles of the error dynamics are $(-3,-6,-12,-24)$ and $(-6,-12)$ respectively; observer gain $\varepsilon = 0.1$ and $(\alpha_1,\alpha_2,\alpha_3)$ chosen in order to have a stable error dynamics; observer discount rate: $\lambda = 20$.

A. Step Response

The Figs. 1, 2 show the step response results of the closed loop system. The reference details are reported on the captions of each figure. The plots showing the observer results are focused only on the initial and most relevant part of simulation, i.e., in which the prediction error is nonzero. We neglect the remaining part since the estimated state follows exactly the real one.

The plots show that, even with a discontinuous step reference on both the outputs, the proposed method preserve the stability of the closed loop system.

In the initial part of Fig. 1b, we can notice that, since the initial velocity is zero, the selector chooses the wrong observer. Nevertheless, after just some milliseconds, at time t_1, since the controller makes the elevation velocity nonzero, the correct observer is selected and never changed again. Since the elevation trajectory lives in the third and forth quadrant, we can imagine the robot attached to the roof. Moreover, since we are requiring compression, the stabilization point is not trivial since the problem is similar to the inverted pendulum.

For the step reference passing from tension to compression showed in Fig. 2, we notice that, instead of inverting the sign of the thrust, the vehicle changes its attitude from up facing to down facing.

B. Smooth Trajectory

The Figs 3, 4, 5, 6 show the behavior of the system following smooth trajectory from an initial to a final output configuration. The plots of the tracking errors show that the proposed controller is able, after a short transient, to perfectly follow the time varying smooth trajectories of class C^3 and C^1 for the elevation and stress, respectively.

In Fig. 5 it is interesting to notice that to pass from tension to compression the vehicle turns upside-down and keeping the thrust always positive. On the other side, in the simulation of Fig. 6 the transition from tension to compression is obtained with the thrust that passes through zero and inverts its sign in order to obtain the same final compressing force of the simulation of Fig. 5. This happens because in the second case the desired trajectory requires zero thrust at a certain moment. Then, since it is not possible to instantaneously turn the vehicle the controller inverts the sign of the thrust in order to provide compression. In the case of vehicles able to provide also negative thrust this is not a problem. While, in the case of robots providing only positive in order to generate feasible trajectories.

C. Sinusoidal Trajectory

In the third groups of simulations we want to show the ability of the presented method to follow a continuously changing trajectory as a sine curve, on both elevation and tension. As we can see in Fig. 7 and 8, the system shows an initial tracking error due to the transient in the observer. However, as soon as the estimation error goes to zero, the tracking error quickly goes to zero as well, i.e., the elevation and stress of the link follow exactly the desired sinusoidal trajectories.

Marco Tognon and Antonio Franchi are with LAAS-CNRS, 7 Avenue du Colonel Roche, 31077 Toulouse CEDEX 4, France. mtognon@laas.fr,antonio.franchi@laas.fr

REFERENCES

[1] M. Tognon and A. Franchi, "Nonlinear observer-based tracking control of link stress and elevation for a tethered aerial robot using inertial-only measurements," in *2015 IEEE Int. Conf. on Robotics and Automation*, Seattle, WA, 2015.

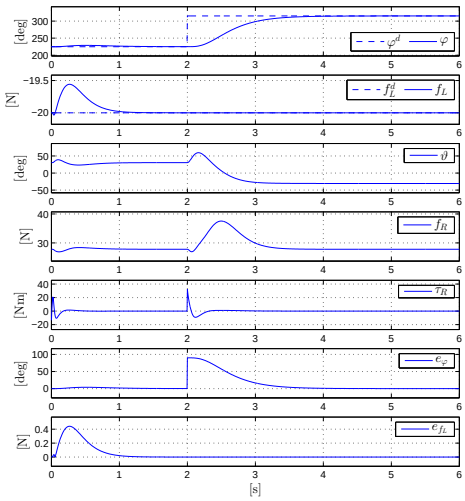

(a) Controller Results: notice that after the transient due to the estimation error, the stress is kept constant even if a step in the elevation is required.

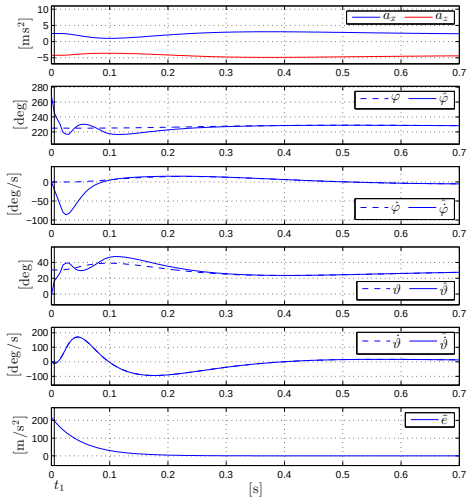

(b) Observer Results: the vertical line, labeled t_1, indicates the instant on which the selector changes observer, from the incorrect to the correct one. After this instant the 'good' observer is never changed again.

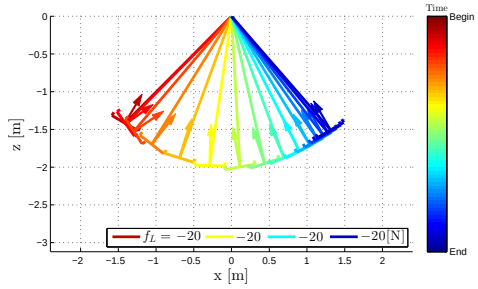

(c) Trajectory visualization.

Fig. 1: The desired elevation trajectory is a discontinuous step from the initial value $\varphi_0^d = 5\pi/4\,[\text{rad}]$ to the final $\varphi_f^d = 7\pi/4\,[\text{rad}]$. While the desired stress is a constant compression, $f_L^d = -20\,[\text{N}]$.

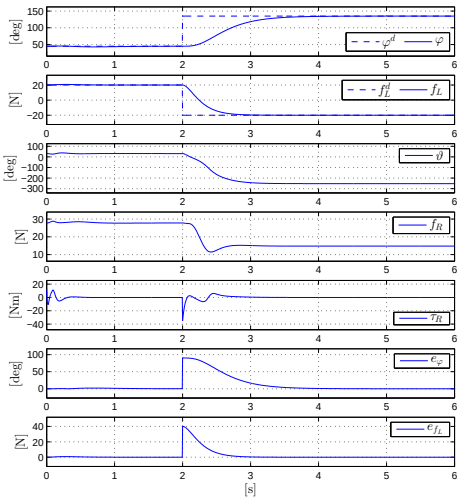

(a) Controller Results: asking an instantaneous transition from tension to compression we can notice a peak on the torque needed to rotate the vehicle as fast as possible in order to provide the compression.

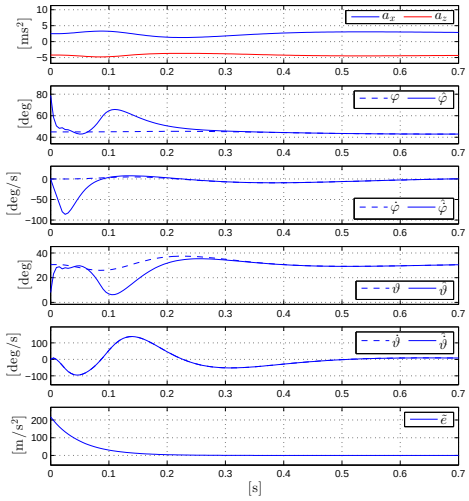

(b) Observer Results.

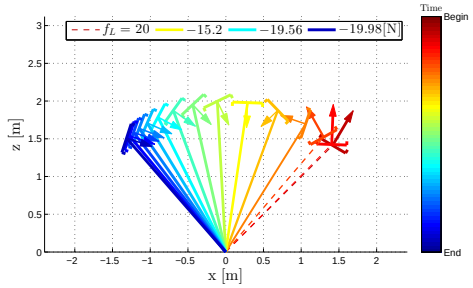

(c) Trajectory visualization.

Fig. 2: The desired elevation trajectory is a discontinuous step from the initial value $\varphi_0^d = \pi/4\,[\text{rad}]$ to the final $\varphi_f^d = 3\pi/4\,[\text{rad}]$. The desired stress trajectory is a step from the initial tension $f_{L\,0}^d = 20\,[\text{N}]$ to the final compression $f_{L\,f}^d = -20\,[\text{N}]$.

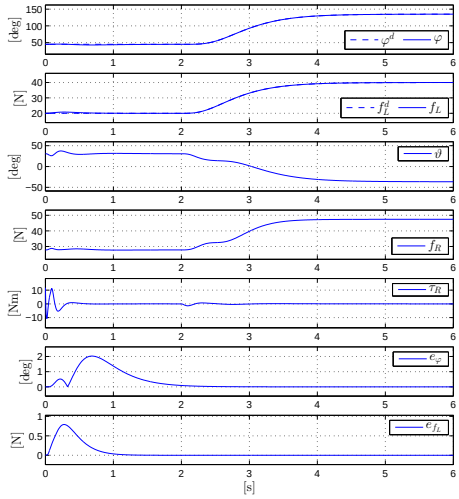

(a) Controller Results.

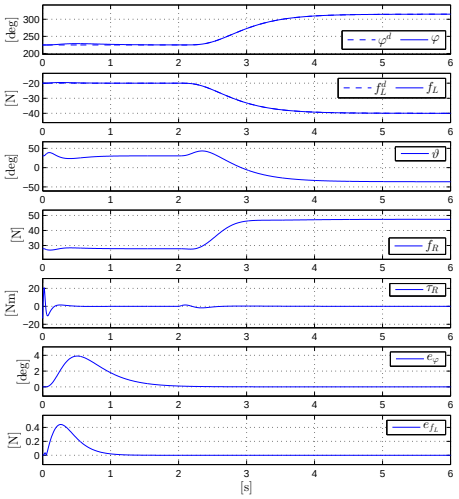

(a) Controller Results.

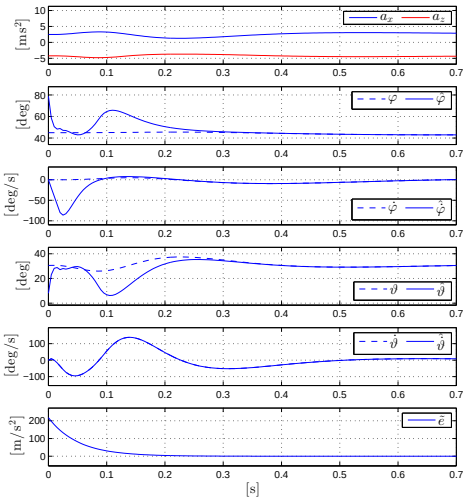

(b) Observer Results.

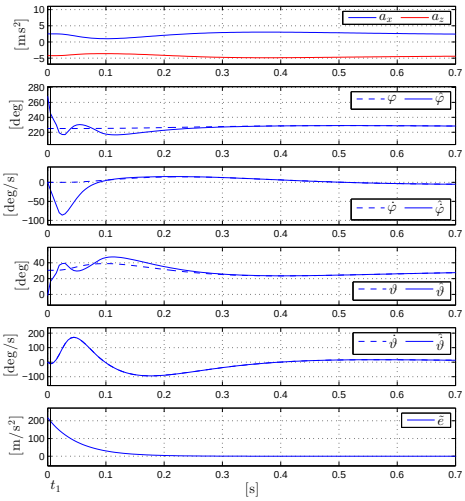

(b) Observer Results.

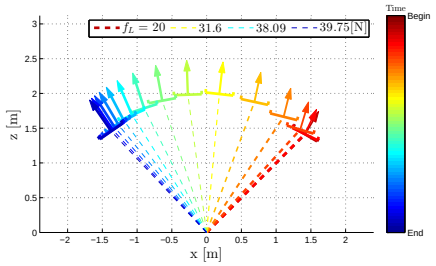

(c) Trajectory visualization.

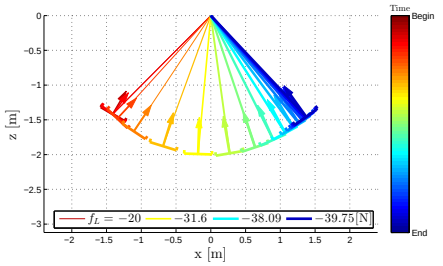

(c) Trajectory visualization.

Fig. 3: The desired smooth elevation trajectory of class C^3 goes from the initial value $\varphi_0^d = \pi/4\,[\text{rad}]$ to the final $\varphi_f^d = 3\pi/4\,[\text{rad}]$. The desired smooth stress trajectory of class C^1 goes from the initial tension $f_{L\,0}^d = 20\,[\text{N}]$ to the final tension $f_{L\,f}^d = 40\,[\text{N}]$.

Fig. 4: The desired smooth elevation trajectory of class C^3 goes from the initial value $\varphi_0^d = 5\pi/4,[\text{rad}]$ to the final $\varphi_f^d = 7\pi/4,[\text{rad}]$. The desired smooth stress trajectory of class C^1 goes from the initial compression $f_{L\,0}^d = -20\,[\text{N}]$ to the final compression $f_{L\,f}^d = -40\,[\text{N}]$.

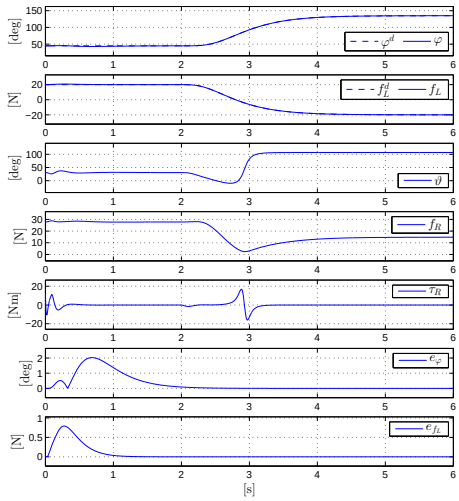

(a) Controller Results.

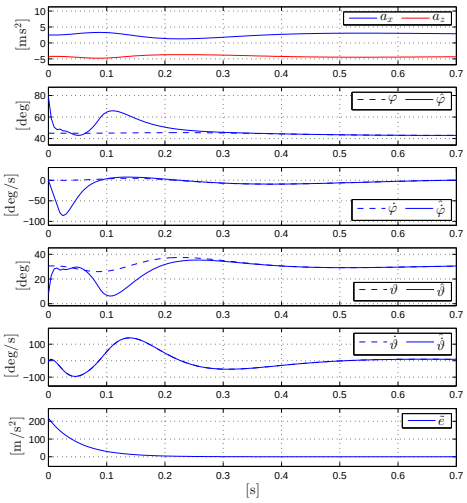

(b) Observer Results.

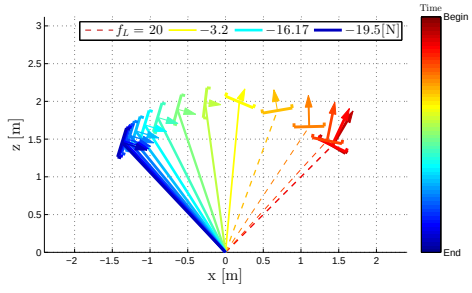

(c) Trajectory visualization.

Fig. 5: The desired smooth elevation trajectory of class C^3 goes from the initial value $\varphi_0^d = \pi/4\,[\text{rad}]$ to the final $\varphi_f^d = 3\pi/4\,[\text{rad}]$. The desired smooth stress trajectory of class C^1 goes from the initial tension $f_{L\,0}^d = 20\,[\text{N}]$ to the final compression $f_{L\,f}^d = -20\,[\text{N}]$.

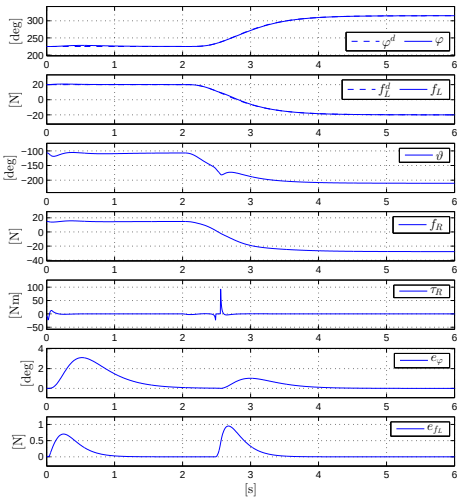

(a) Controller Results.

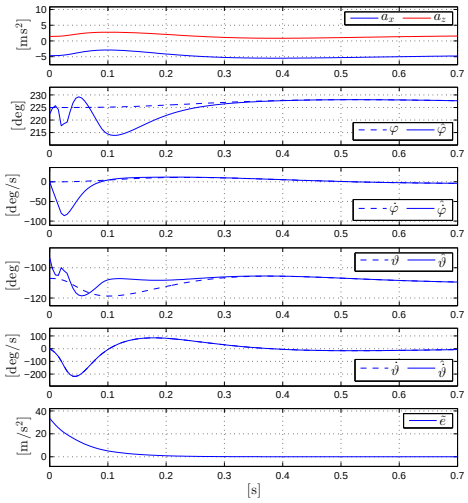

(b) Observer Results.

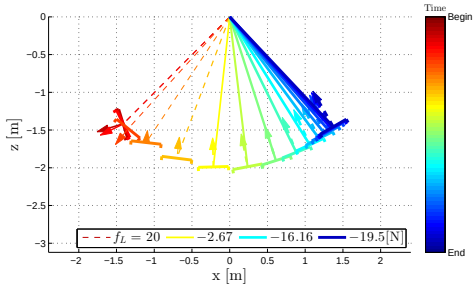

(c) Trajectory visualization.

Fig. 6: The desired smooth elevation trajectory of class C^3 goes from the initial value $\varphi_0^d = 5\pi/4\,[\text{rad}]$ to the final $\varphi_f^d = 7\pi/4\,[\text{rad}]$. The desired smooth stress trajectory of class C^1 goes from the initial tension $f_{L\,0}^d = 20\,[\text{N}]$ to the final compression $f_{L\,f}^d = -20\,[\text{N}]$.

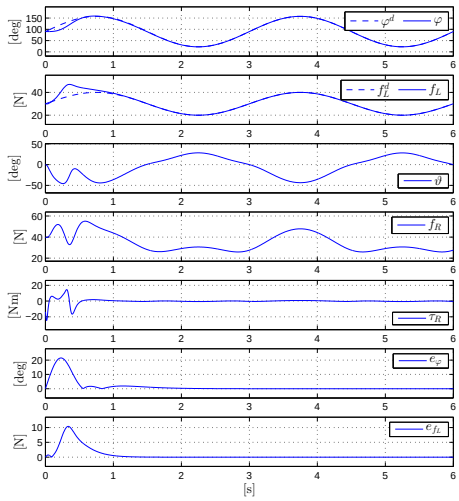

(a) Controller Results.

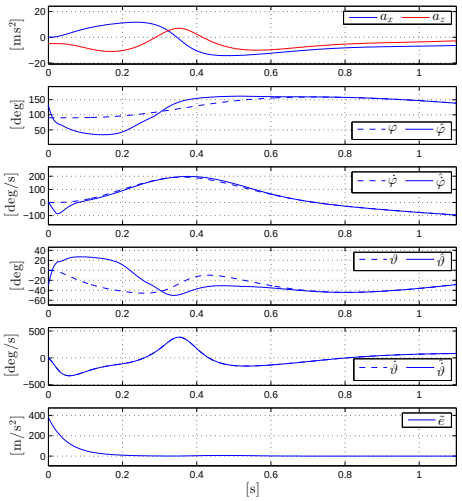

(b) Observer Results.

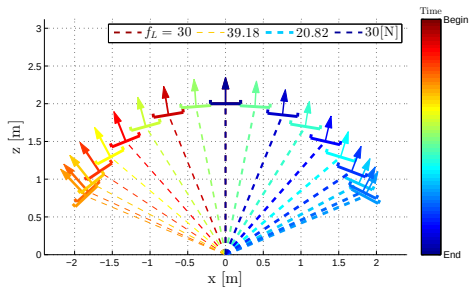

(c) Trajectory visualization.

Fig. 7: The desired elevation trajectory is a sine curve from the minimum value $\varphi^d_{min} = \pi/8\,[\text{rad}]$ to the maximum $\varphi^d_{max} = 7\pi/8\,[\text{rad}]$ with period $T_\varphi = 3\,[\text{s}]$. The desired stress is sinusoidal from the minimum tension $f^d_{L\,min} = 20\,[\text{N}]$ to the maximum $f^d_{L\,min} = 40\,[\text{N}]$ with period $T_{f_L} = 3\,[\text{s}]$.

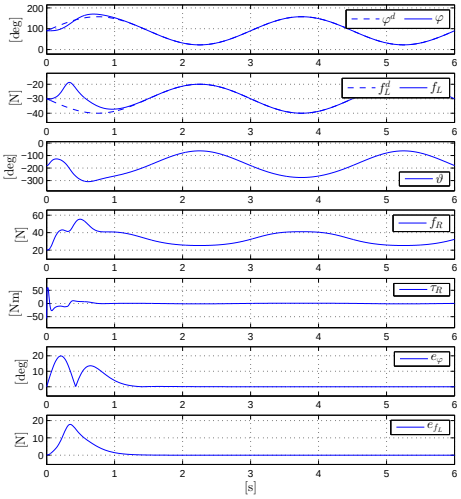

(a) Controller Results.

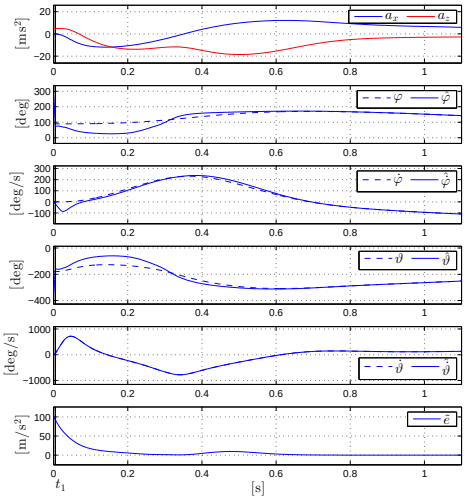

(b) Observer Results.

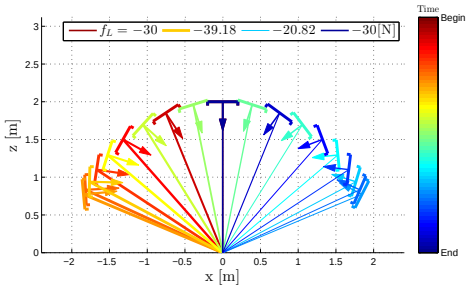

(c) Trajectory visualization.

Fig. 8: The desired elevation trajectory is a sine curve from the minimum value $\varphi^d_{min} = \pi/4\,[\text{rad}]$ to the maximum $\varphi^d_{max} = 3\pi/4\,[\text{rad}]$ with period $T_\varphi = 3\,[\text{s}]$. The desired stress trajectory is sinusoidal from the minimum compression $f^d_{L\,min} = 20\,[\text{N}]$ to the maximum tension $f^d_{L\,min} = 40\,[\text{N}]$ with period $T_{f_L} = 3\,[\text{s}]$.